JOURNAL OF MATERIALS SCIENCE 27 (1992) 1113–1120

Influence of microstructure and strain rate on the compressive strength of whisker-reinforced ceramic matrix composites

J. LANKFORD
Materials and Mechanics Department, Southwest Research Institute, PO Drawer 28510, San Antonio, TX 78228, USA

The compressive strength of pyroceramic reinforced with a wide variety of SiC whiskers was characterized at loading rates which range from quasi-static to dynamic. It was found that strength is inversely related to whisker size, and essentially strain rate insensitive. The same strain rate independence was obtained for unreinforced matrix, but the strength of the latter lies below that for small ($\leqslant 1$ μm diameter) whisker-reinforced composites, and above that for large ($\gtrsim 3$ μm diameter) whisker material. Whisker/crack interaction and (to a lesser extent) whisker pull-out seem to be responsible for the beneficial influence of small whiskers, while the apparently detrimental large whiskers serve as microcrack-nucleating inclusions.

1. Introduction

The combined strengthening and toughening of ceramic matrices by the introduction of ceramic whiskers is receiving considerable current attention [1]. However, most of this effort has been devoted to tensile or flexural loading conditions, for which a variety of whisker–matrix interactions (microcracking process zone; phase transformation-induced residual stress field; crack deflection; crack bridging/whisker pullout) have been identified [2, 3]. It has been shown that these interactions are quite promising [1], and models are being developed to guide optimization of composite architecture in terms of these mechanisms.

On the other hand, almost no consideration has been given to the performance and underlying constituent interactions of whisker-reinforced ceramics subject to compressive stresses. Because it is thought that this family of composites may be particularly useful in applications involving wear and impact [1], it clearly is relevant to try and understand its behaviour under compression over a wide range in rate of loading. Previously, the compressive strength of a SiC fibre-reinforced silicon nitride matrix had been determined under both quasi-static and dynamic (near impact) strain rates. It was found that the whiskers degraded the strength of the matrix under quasi-static conditions, but at strain rates in excess of about 1000 s^{-1}, the strength began to increase at an extremely rapid rate (i.e. relative to rising strain rate), and the composite versus matrix strength differential observed at lower rates of loading disappeared. The objective of the present study was to expand this limited base of knowledge by investigating a different class of matrix, prepared in two fundamentally different microstructural variants, reinforced with a wide variety of whisker types.

2. Material

The material chosen for study was fabricated by United Technologies Research Center (UTRC). It was prepared as described in detail by Brennan [4], and briefly as follows. Lithium aluminosilicate powder (denoted LAS-I by UTRC) was hot-pressed with several commercially available SiC whiskers; all composites were formulated to contain 30 vol % whiskers. In the as-pressed state, the matrix was glassy. A drastically different microstructure was produced by heat-treating the material in argon at 900 °C for 24 h, which crystallized the material in the form of 0.5–2 μm grains of β-spodumene/silica solid solution phase in the β-quartz crystal structure. The dimensions of the whiskers, and the tensile mechanical properties [4] of the resultant composites and the two matrix variants (glassy and crystalline, denoted by material postscripts 1 and 2, respectively) are given in Table I. Also listed is a closely related pyroceram, Corning 9606, in the ceramed state. Although equivalent tensile strength and toughness were not known for the latter, its compressive behaviour had been previously characterized [6], and will be compared with that of the present composites; unfortunately, no pure LAS-I, in either the as-pressed or ceramed condition, was available for compression testing. However, Corning 9606 and UTRC LAS-I are sufficiently similar chemically and microstructurally that it seems highly likely that they would share equivalent compressive response.

The microstructures of the four basic composites are shown in Fig. 1. In these low-magnification views, the generally heterogeneous whisker dispersion is evident; only the T2 material is relatively homogeneous. It should be emphasized that similar dispersions prevail in the as-pressed (glassy) state as well. The relative sizes and aspect ratios of the individual whiskers are shown in Fig. 2. In addition to the whiskers,

TABLE I Material parameters

Material	Whisker diameter (μm)	Condition	Three-point bend flexural strength (MPa)	Fracture toughness (MPa $m^{1/2}$)
A1	< 0.7[a]	As-pressed	400	4.73
A2		Ceramed	393	4.44
T1	1.0[b]	As-pressed	358	3.82
T2		Ceramed	373	4.06
AMI 1	3.0[c]	As-pressed	166	2.83
AMI 2		Ceramed	193	2.83
LANL 1	5–8[d]	As-pressed	110	2.29
LANL 2		Ceramed	103	2.24
LAS 1	–	As-pressed	83	0.80
LAS 2	–	Ceramed	138	1.00
Pyroceram[e]	–	Ceramed	–	–

[a] Arco SC-9.
[b] Tokai TWS-400.
[c] American Matrix Inc.
[d] Los Alamos National Laboratory.
[e] Corning 9606.

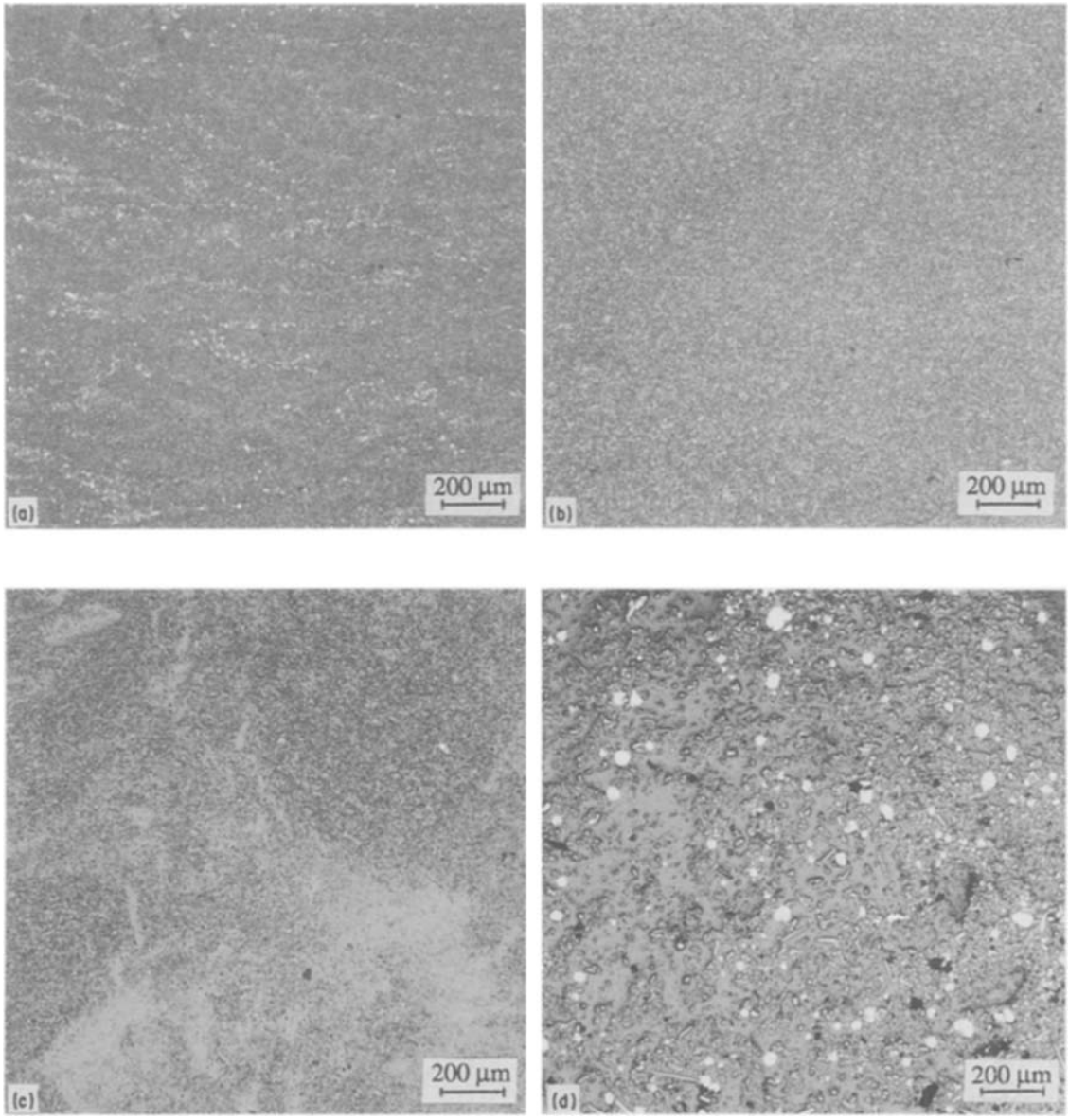

Figure 1 Macroscopic views of relative composite heterogeneity; compression axis horizontal, lying within hot-pressing plane. (a) A2, (b) T2, (c) AMI 2, (d), LANL2.

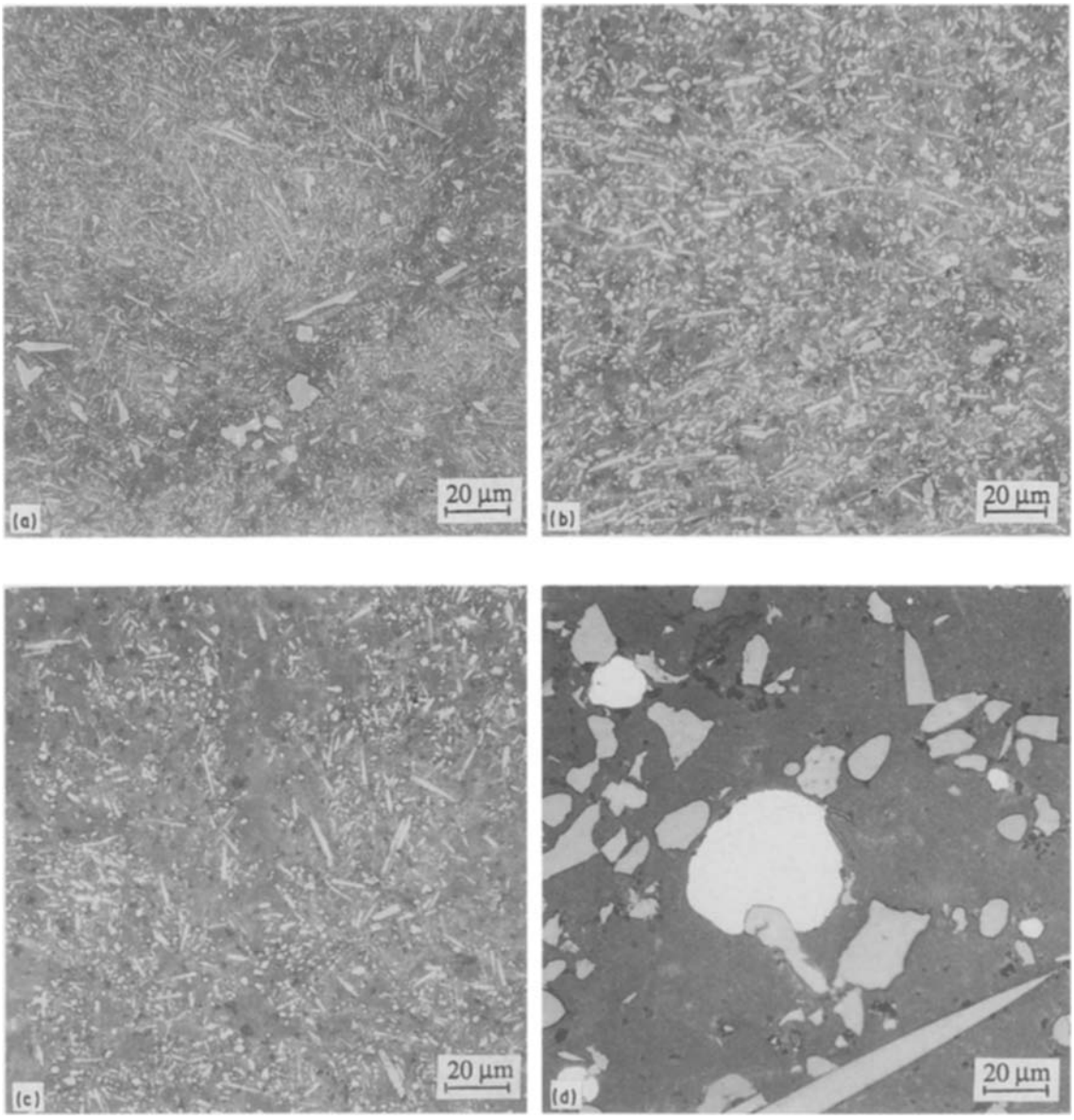

Figure 2 Microscopic views of whisker size, shape, and distribution; compression axis horizontal, lying within hot-pressing plane. (a) A2, (b) T2, (c) AMI 2, (d) LANL2.

considerable particulate debris is included in the microstructures. Surface characterization by Brennan [4] has shown that all four of the whisker variants are covered with carbon-rich films. In addition, the Arco and LANL whiskers are very smooth; the Tokai whiskers are fairly smooth, but wavy in profile; and the AMI whiskers are very rough in surface morphology.

3. Experimental procedures

Cylindrical specimens for compression testing were sectioned from blanks provided by UTRC, with the compression axis lying within the hot-pressing plane (Figs 1 and 2). The samples, as well as high-strength alumina loading platens, were ground and lapped parallel to within 5 μm across the 6.5 mm width of the 13 mm long specimens.

Using a standard, but carefully aligned, servo-controlled hydraulic test machine, strain rates ranging from approximately 10^{-4}–$2\,s^{-1}$ were realized. At the lower of these, it was possible to utilize acoustic emission to detect the onset and monitor the development of microcracking. The acoustic emission transducer was resonant at 160 kHz, and its input was filtered to provide a sampling domain of 100 kHz–1 MHz.

Dynamic compression tests were performed using a split Hopkinson pressure bar (SHPB), which yielded strain rates, $\dot{\varepsilon}$, derived from the stress rate, $\dot{\sigma}$, of the incident stress pulse according to $\dot{\varepsilon} = \dot{\sigma}/E$, where E is the elastic modulus. The rapidity of these tests ($< 10\,\mu s$) precluded the implementation of acoustic emission.

Failed specimens consisted of a multitude of microscopic fragments. Samples of these were mounted and coated with gold for scanning electron microscopy (SEM). In addition, an effort was made to monitor the development of microcracking by studying damaged but unfailed specimens. This was accomplished by loading samples quasi-statically ($\dot{\varepsilon} \simeq 10^{-4}\,s^{-1}$) to stress levels as high as 95% compressive strength, σ_c,

and then rapidly unloading them to prevent failure. Because observation by SEM failed to reveal microcracking, the specimens were reloaded to a compressive stress of about 0.75 σ_c, held at that level, and replicated to record the presence of previously nucleated microcracks which might be opened up by the moderate applied load.

4. Results

4.1. Mechanical behaviour

Stress–strain response was similar for both as-pressed and ceramed composites, examples of which are shown in Figs 3 and 4 for both Arco and LANL whisker-reinforced material. For specimens whose strength exceeded approximately 1200 MPa, a clearly defined yield point was measured (Fig. 3); this value varied from 1250–1400 MPa for A1, A2, T1, and T2. On the other hand, the deformation of AMI and LANL based composites was linear elastic (Fig. 4). In all cases, acoustic emission was not detected until failure was imminent, so that the acoustic emission stress level, σ_{AE}, was nearly equal to σ_c. The latter behaviour was remarkably different from that of pure Pyroceram, shown in Fig. 5. Here it is evident that although the ceramic yields in a fashion similar to that of the stronger composites, acoustic emission occurs early

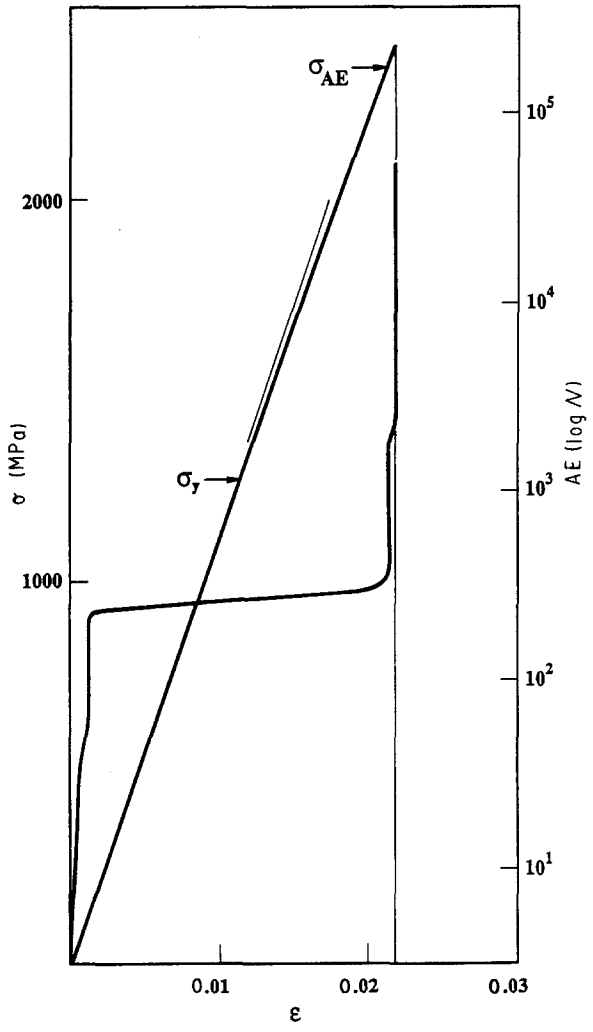

Figure 3 Stress and acoustic emission versus strain for A2 at $\dot{\varepsilon} = 3.2 \times 10^{-4} s^{-1}$.

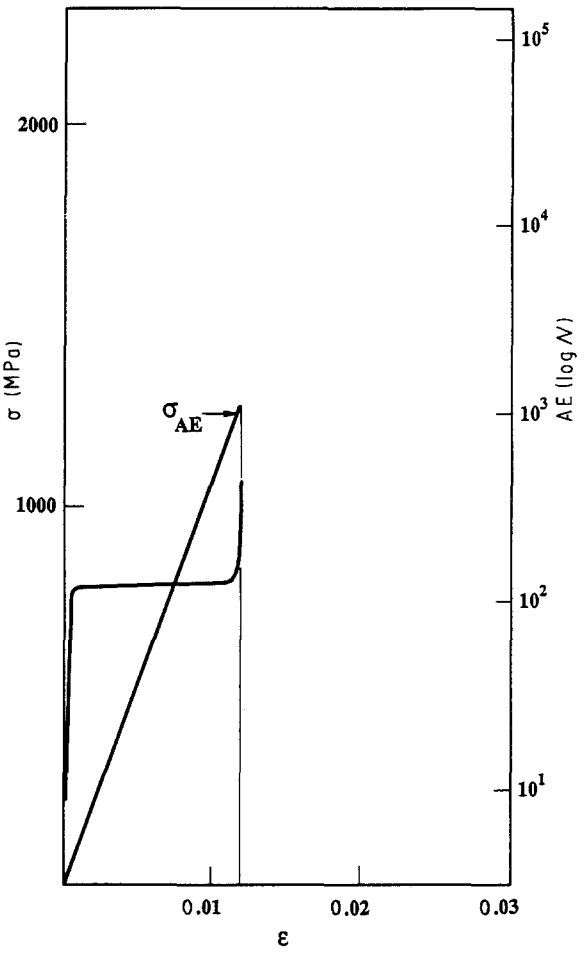

Figure 4 Stress and acoustic emission versus strain for LANL2 at $\dot{\varepsilon} = 2.8 \times 10^{-4} s^{-1}$.

(relative to σ_c) and abundantly. For the composites, there is no correlation between σ_{AE} and σ_y.

Strength as a function of strain rate for all the materials is summarized in Figs 6 and 7. Because the matrix material was studied in the ceramed state, it is included with the ceramed composites (Fig. 7). The materials clearly are basically strain-rate insensitive over the range of the tests, so that it is possible, for purposes of comparison, to consider each composite as possessing an approximately singular strength.

Thus, for both matrix microstructures, the Tokai and Arco (smaller whisker) variants are significantly stronger than the AMI and LANL whisker-reinforced material. The base pyroceram possesses a strength (Fig. 7) intermediate to that of A2/T2 and AMI2/LANL2. In all cases, the compressive strength of the as-pressed composites exceeds that of corresponding ceramed variants. Furthermore, this superiority is most marked for the stronger materials, as shown along the left-hand edge of Fig. 7; here the relative declines in strength effected by the glassy-to-crystalline transformation are indicated for $\dot{\varepsilon} \simeq 10^{-5} s^{-1}$. While the strength of Tokai and Arco reinforced material drops precipitously, that of the LANL reinforced material is virtually unaffected.

4.2. Fracture characteristics

Characterization of the damage state in specimens loaded nearly to failure proved difficult. Only for

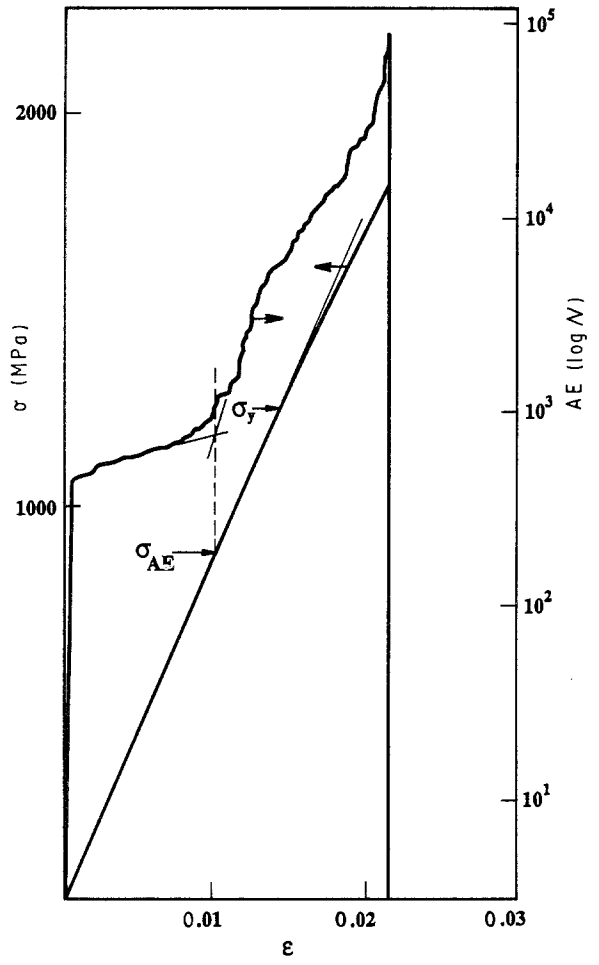

Figure 5 Stress and acoustic emission versus strain for Pyroceram at $\dot{\varepsilon} = 1 \times 10^{-4} s^{-1}$.

LANL2 material was it possible to detect microcracks, some of which are shown in Fig. 8, representing a specimen loaded to 95% of its nominal compressive strength at a strain rate of approximately $10^{-4} s^{-1}$. Based on Fig. 8a, it appears that an axial microcrack has nucleated at the surface of a large whisker, as indicated by the arrow. On the other hand, once a crack in this system has nucleated, it seemingly does not subsequently experience significant interaction with those whiskers which it may encounter (Fig. 8b).

The preceding inferences are strongly supported by SEM study of the fracture surfaces of specimen fragments, and a number of other factors are thereby revealed. Fig. 9, for example, shows the fracture modes characteristic of quasi-static loading rates for two extremes in strength, i.e. for Arco and LANL reinforced material, with the matrix in both the as-pressed and ceramed conditions. For both whisker variants, fracture of the as-pressed material was surprisingly ductile, almost "viscous" (Fig. 9a and c), while in the ceramed state, failure occurred in an obviously brittle fashion (Fig. 9b and d). Fracture of the Arco composite evinces both fibre pull-out, in the form of fibre-shaped (rounded triangular) holes, and crack deflection around fibres (Fig. 9a and b); similar features were observed for T1 and T2 material. No such pull-out occurred for either the LANL (Fig. 9c and d) or the AMI composite.

At high strain rates, the fracture appearances were similar, except that the "viscous" nature of as-pressed material was suppressed, and the fracture became much more "brittle" (Fig. 10), resembling that of the ceramed variants (Fig. 9b). Whisker pull-out was still observed for the Arco and Tokai reinforced LAS, and crack deflection by whiskers lying in the crack plane (Fig. 10) was quite pronounced.

A few specific details seem worthy of mention. The "viscous" fracture mode characteristic of as-pressed material at lower rates of loading is clearly evident in Fig. 11. The appearance is that of ductile hole growth by the formation of local tensile ligaments which fail by necking. It is hardly necessary to observe that this is an uncommon failure mechanism for any ceramic

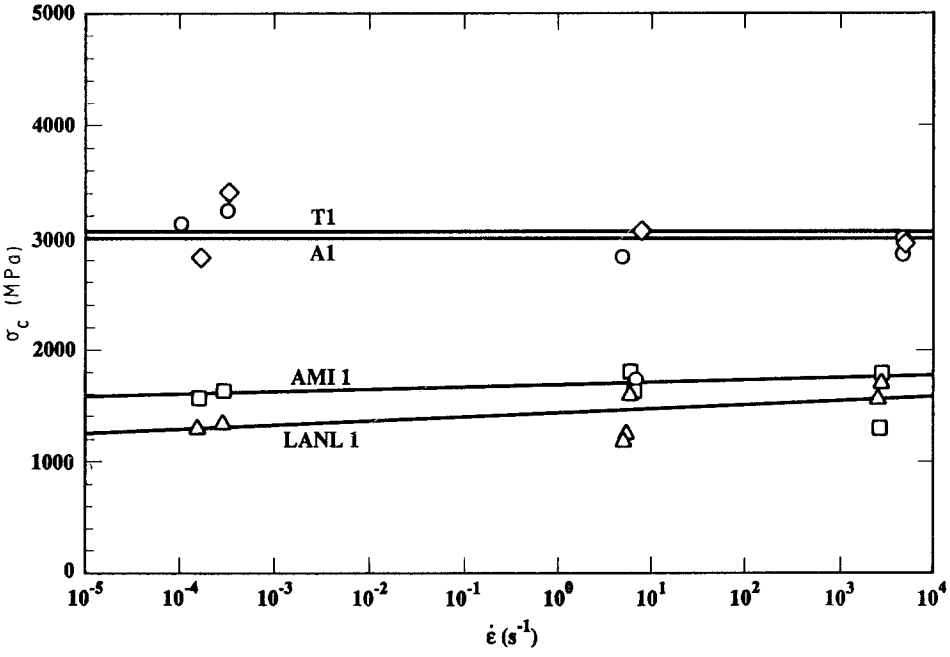

Figure 6 Compressive strength versus strain rate for as-pressed composites.

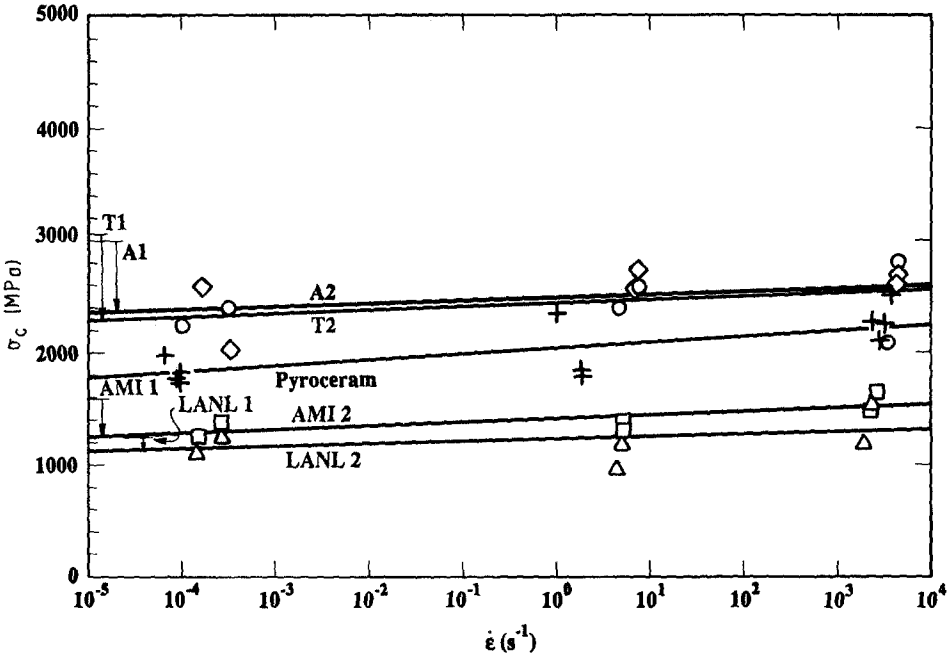

Figure 7 Compressive strength versus strain rate for ceramed composites and Pyroceram.

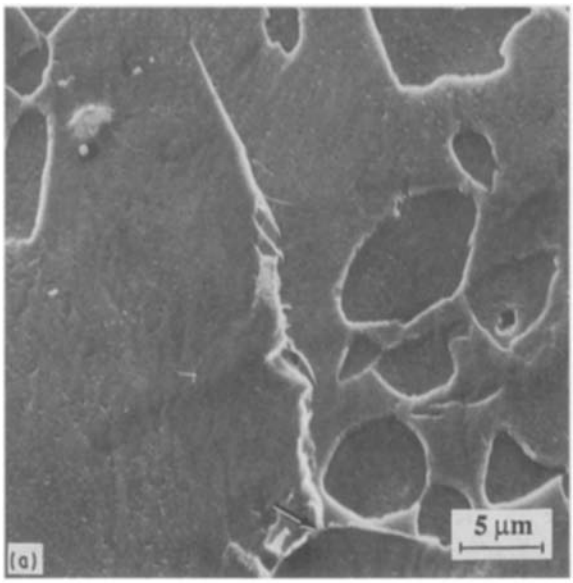

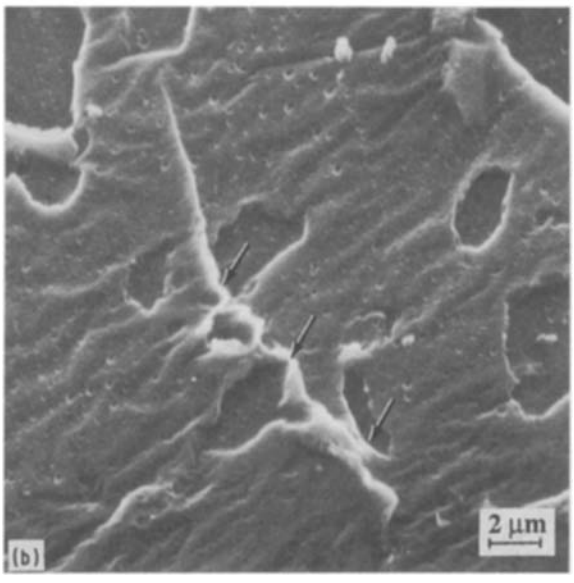

(even a "glassy" one) under quasi-static, ambient conditions.

Finally, a frequently observed fractographic feature in the LANL and AMI composites was the presence of matrix microcracks associated with whiskers, with the crack plane oriented parallel to the whisker axis. Fig. 11b shows such a microcrack nucleated at the whisker–matrix interface, the conformation of the crack being that of a classic half-penny.

5. Discussion

Probably the most striking aspect of the present results is the range of strength values obtained, and the fact that they tend to lie above and below the strength of pyroceram material, which is extremely similar in chemistry and microstructure to the matrix material. It is possible to rationalize this behaviour in terms of the specific influence of the reinforcing whiskers, which can manifest themselves in several ways, depending on their relative size, spacing, and ability to interact with the matrix.

For example, it is clear from the acoustic emission results that the presence of the Arco and Tokai whiskers serves to suppress the strong tendency of the matrix to damage itself by prolonged pre-failure (recall Figs 3 and 5) microfracture. Although some evidence of whisker pull-out was seen, this cannot be the origin of the suppression of microcrack initiation, because the frictional pull-out mechanism presupposes the existence of a whisker-bridged matrix crack. Thus, it seems much more likely that the whiskers retard the onset of crack nucleation through a network of residual stresses generated by whisker–matrix

Figure 8 Early stages of compressive microfracture in LANL2, $\dot{\varepsilon} \simeq 10^{-4} s^{-1}$, $\sigma = 0.95\,\sigma_c$; compression axis vertical. (a) Crack nucleated at large whisker (arrow). (b) Crack non-interaction with adjacent whiskers (arrows).

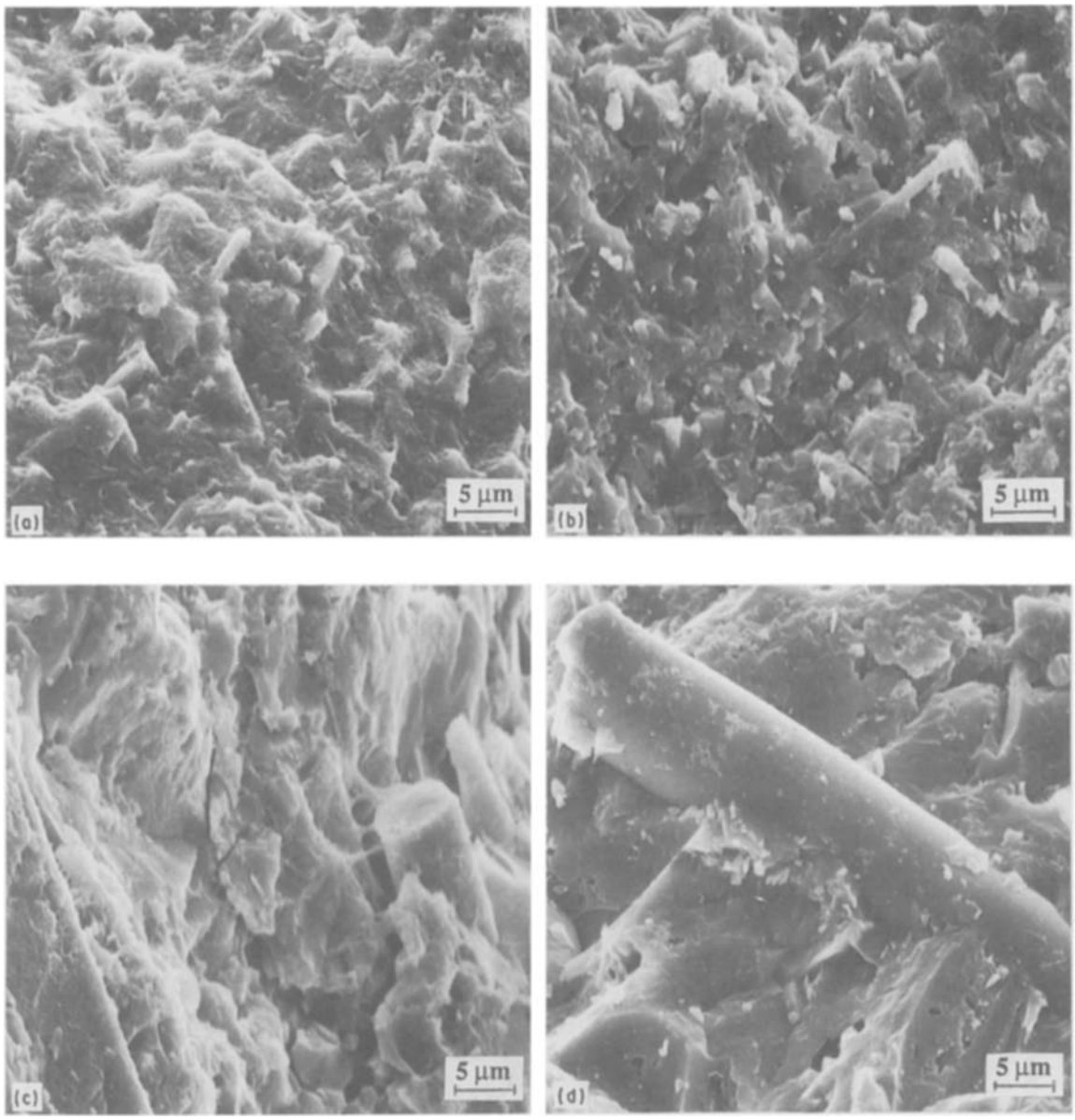

Figure 9 Fracture surfaces, Arco versus LANL whiskers, as-pressed and ceramed, $\dot{\varepsilon} \simeq 10^{-4}\,s^{-1}$. (a) A1, (b) A2, (c) LANL1, (d) LANL 2.

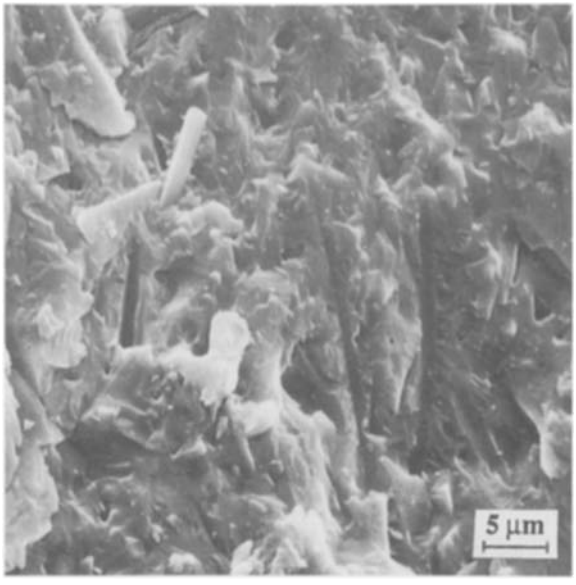

Figure 10 Fracture surface of A1 at $\dot{\varepsilon} \simeq 2000\,s^{-1}$. Note evidence of crack deflection, in the whisker-shaped crevices left by whiskers attached to the mating surface.

thermal expansion mismatch. The concept of a network is based on the fact that for the same whisker volume fraction, the whisker/matrix "unit cell" will be much smaller than that of composites reinforced with the larger AMI and LANL whiskers. In the latter case, the whiskers are sufficiently far apart (Fig. 9d) that large volumes of matrix are basically unreinforced.

Moreover, it was shown (Fig. 11b) that the large whiskers actually are detrimental, in that they are potent crack nuclei. Under compressive loading, being much harder than the matrix, they act as micro-indentors, producing axially oriented (locally) tensile microcracks. This would also be the case for the smaller Arco and Tokai whiskers as well, but the microcracks would be smaller, because the size of the local tensile field would scale with whisker diameter.

The hypothesis that residual stresses are responsible for the good (relative to pyroceram) performance of the Arco and Tokai whisker-reinforced material is supported by the fact that it is for these systems that the greatest strength differential is observed upon heat

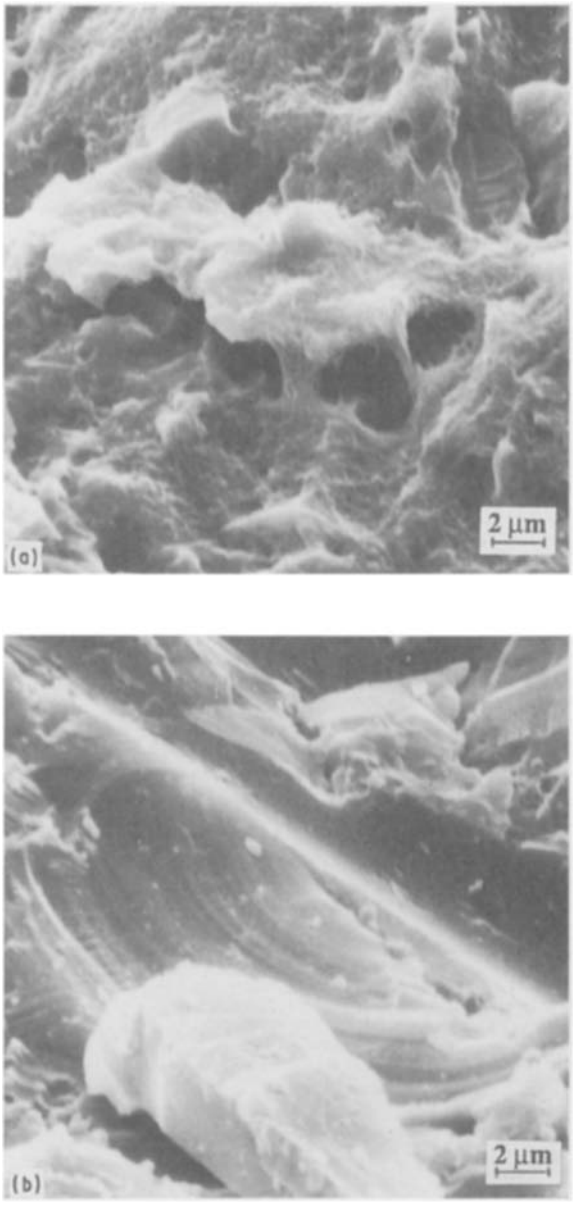

Figure 11 (a) Viscous fracture mode in A1 tested at $\dot{\varepsilon} \simeq 10^{-4} s^{-1}$, (b) Whisker-initiated microcracking in LANL1 at $\dot{\varepsilon} \simeq 10^{-4} s^{-1}$.

treating the as-pressed material to the ceramed state. This process would in no way change whiskers, but it would tend to alter, evidently in the compressive direction, the global residual stress field. Similarly, the minimal strength differential for as-pressed and ceramed AMI and LANL whisker composites suggests that the dominant role is played by the crack nucleating "inclusion" nature of the large whiskers.

Although the apparent "viscous" fracture capability of the as-pressed material is surprising and interesting, it does not seem very important, compared to residual stresses and whisker crack nucleating capabilities. If it were significant, it would be expected that as the strain rate increased, the strength of the as-pressed material would rise or fall versus that of the ceramed material. Clearly (Figs 3 and 4), that is not the case.

The ceramed-state fracture features observed in these experiments are qualitatively similar to those characterized by Brennan [4] for identical material failed in flexure. His conclusions regarding the relative roles of whisker pull-out and crack path tortuosity are borne out, reinforcing the fact that the compressive failure mode is in reality a series of more-or-less simultaneous local tensile microcrack nucleation events, producing an ensemble of axial cracks which coalesce to produce failure.

The absence of a dynamic strain-rate strengthening effect in the present experiments stands in stark contrast to the intense rate sensitivity obtained [5] in SHPB tests of SiC whisker-reinforced, as well as unreinforced, hot-pressed Si_3N_4. Considering these two extreme cases, it is evident that the presence of reinforcing whiskers does not significantly affect dynamic response; rather, the latter must be understood as a function of the matrix phase alone. This is not true for fibre-reinforced ceramics (such as SiC fibre-reinforced LAS [6]), in which case the micromechanics of dynamic failure are remarkably different for the composite versus the matrix.

Acknowledgements

The author is grateful for the support of the Office of Naval Research under Contract no. N00014-84-C-0213. The kind provision of the whisker-reinforced blanks by J. J. Brennan, UTRC, is gratefully appreciated, as is the careful experimental work by A. Nicholls.

References

1. S.-T. BULJAN, A. E. PASTO and H. J. KIM, *Amer. Ceram. Soc. Bull.* **68** (1989) 387.
2. G. C. WEI and P. F. BECHER, *ibid.* **64** (1985) 298.
3. P. F. BECHER, *Acta Metall.* **34** (1986) 1985.
4. J. BRENNAN, "Interfacial Studies of Whisker Reinforced Ceramic Matrix Composites," Annual Report R89-917894-1, AFOSR Contract. No. F49620-88-C-0062, 31 May, 1989.
5. J. LANKFORD and C. R. BLANCHARD, *Mater. Sci. Engng*, in press.
6. J. LANKFORD, *Ceram. Engng Sci. Proc.* **9** (1988) 843.

Received 29 January
and accepted 25 February 1991